



Reliability Assessment of Single-phase PV Inverters

Peyghami, Saeed; Davari, Pooya; Blaabjerg, Frede; Abdelhakim, Ahmed

Published in:

Proceedings of 2019 10th International Conference on Power Electronics and ECCE Asia (ICPE 2019 - ECCE Asia)

Publication date:

2019

Document Version

Accepted author manuscript, peer reviewed version

[Link to publication from Aalborg University](#)

Citation for published version (APA):

Peyghami, S., Davari, P., Blaabjerg, F., & Abdelhakim, A. (2019). Reliability Assessment of Single-phase PV Inverters. In *Proceedings of 2019 10th International Conference on Power Electronics and ECCE Asia (ICPE 2019 - ECCE Asia)* (pp. 3077-3083). [8796895] IEEE Press. International Conference on Power Electronics <https://ieeexplore.ieee.org/document/8796895>

General rights

Copyright and moral rights for the publications made accessible in the public portal are retained by the authors and/or other copyright owners and it is a condition of accessing publications that users recognise and abide by the legal requirements associated with these rights.

- Users may download and print one copy of any publication from the public portal for the purpose of private study or research.
- You may not further distribute the material or use it for any profit-making activity or commercial gain
- You may freely distribute the URL identifying the publication in the public portal -

Take down policy

If you believe that this document breaches copyright please contact us at vbn@aub.aau.dk providing details, and we will remove access to the work immediately and investigate your claim.

Reliability Assessment of Single-phase PV Inverters

Saeed Peyghami¹, Ahmed Abdelhakim², Pooya Davari¹, Frede Blaabjerg¹

¹Department of Energy Technology, Aalborg University, Aalborg, Denmark
{sap, pda, fbl}@et.aau.dk

²Department of Electrical Systems, ABB Corporate Research Center, Västerås, Sweden
ahmed.abdelhakim@se.abb.com

Abstract— This paper investigates the reliability of two types of single-phase Photo-Voltaic (PV) inverters, which are a quasi-Z-Source Inverter (qZSI) and a conventional two-stage boost-based inverter. The converters reliability is estimated by employing a mission-profile based reliability assessment approach modeling the wear-out failure of fragile components, i.e., capacitors and semiconductor devices. The obtained results reveal that the conventional two-stage inverter has better reliability compared to the qZSI due to the higher voltage and current stresses on qZSI components. Furthermore, the impact of PV array configuration on the Shoot Through (ST) state of the qZSI and consequently on its reliability is illustrated. The analysis shows that a suitable PV array configuration can improve the qZSI reliability.

Index term— Reliability, wear-out, quasi-Z-source inverter, boost converter, PV inverter, shoot through.

I. INTRODUCTION

Moving towards carbon-free energy technologies has intensified the importance of the renewable energies in the last few decades. It can alleviate the global warming effects due to the emission suppressions and maintaining its percentage towards the lowest limit. Among the different renewable energy resources, the solar Photo-Voltaic (PV) power is the fastest growing energy source due to prices falling and governmental policies [1]. Power electronics technology plays a crucial role in energy conversion process of PV systems. It may though pose to some challenges in terms of design and control aspects. Therefore, numerous efforts have been carried out to control and implement different PV converter structures. Recent investigations have elaborated that using more optimized power converter structures ensures high efficiency and reliability in terms of design and operation [2], [3].

The energy utilization of PV sources implies the use of a power conditioning stage, in which a voltage source inverter (VSI) is commonly used. This VSI requires a sufficient dc-link voltage in order to meet the ac side requirements. Since this is not always feasible, i.e. having a sufficient dc-link voltage, an additional boosting stage is mandatory in order to regulate the PV output voltage, resulting in a two-stage architecture. Alternatively, single-stage impedance-source inverters can be utilized for PV applications where the boost capability can be obtained within the inversion operation [4]–[6]. Impedance source inverters have been experiencing a fast evolution since the

first release of the classical Z-Source Inverter (ZSI) in 2003 [4], [5]. Among the abundant structures of the ZSI, the quasi-ZSI (qZSI), is commonly used due to its simple structure and continuous input current [7], [8]. The qZSI has been studied for many applications, such as PV systems [9], [10], energy storage systems [11], and electric vehicles [12]. Therefore, its reliability performance gains high of interest recently. For instance, the reliability of the quasi-Z-Source Series Resonant DC-DC Converter (qZSSRC) as a PV micro-inverter (300 W) is studied based on physics-of-failure and mission profile based analysis [13]. However, this family of inverters has not been compared to the conventional alternative, i.e., two-stage inverters in terms of reliability.

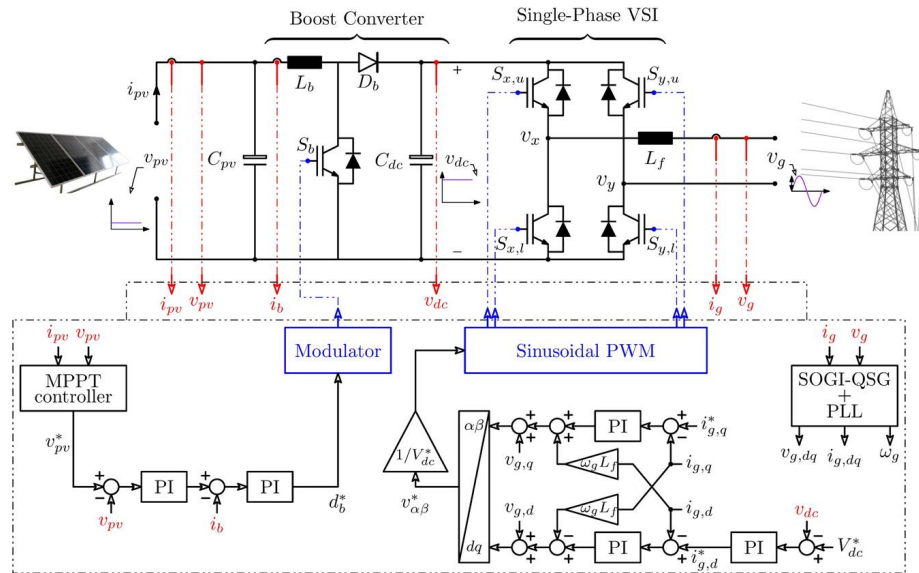
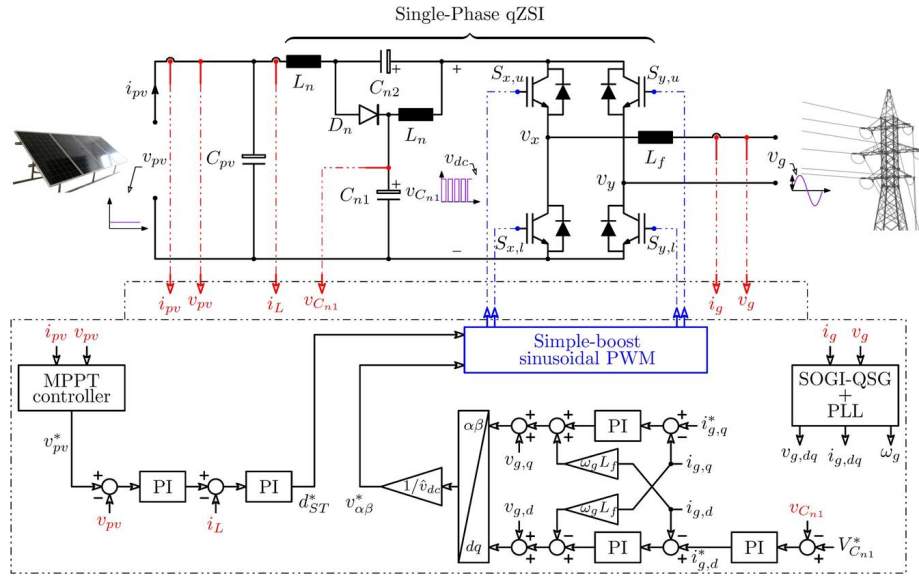
This paper investigates this issue and reveals the reliability performance of a single-phase qZSI in comparison with the conventional two-stage boost-based inverter for PV applications (5 kW). The present study provides a comprehensive insight to identify weak links of qZSI compared to the conventional inverter in order to enhance its reliability performance. In the following, the PV inverter structures and PV array configurations are presented in Section II. Section III describes the reliability prediction procedure. The comparative assessment is provided in Section IV. Finally, the outcomes are summarized in Section V.

II. PV INVERTER STRUCTURES

In this study, two single-phase PV inverters are considered including qZSI and conventional inverter as shown in Fig. 1 and Fig. 2 respectively. Furthermore, two types of PV arrays are employed as a prime-energy source for both inverters with the specifications summarized in Table I. The climate mission profile including solar irradiance (I_{rr}) and ambient temperature (T_a), which is utilized in this study, is shown Fig. 3.

A. Single-Phase qZSI

The structure of the single-phase qZSI is shown in Fig. 1, in which the PV power is feeding the B4-bridge through an impedance network. This impedance network comprises two inductors, two capacitors, and a diode. Such impedance network allows the employed B4-bridge to utilize an additional switching state, which is called Shoot Through (ST) state. During the ST state, all the switches in any or both phase-legs are turned ON simultaneously, under which the B4-bridge is equivalent to a short circuit and the DC link voltage (V_{dc}) is equal to



zero. On the other hand, during any non-ST state, the B4-bridge is equivalent to a current source. Notably, proper control of the ST state duty cycle controls the peak DC link voltage to be larger than or equal to the input voltage (V_{PV}).

Table I: PV arrays parameters

Parameter	Symbol	Array I	Array II
Panel rated power	$P_r (W)$	315	315
Open circuit voltage	$V_{oc} (V)$	51.98	58.22
Short circuit current	$I_{sc} (A)$	8.28	7.38
MPPT voltage	$V_m (V)$	41.73	47.52
MPPT current	$I_m (A)$	7.59	6.62
Voltage temp. coeff.	$\alpha (\%/K)$	-0.33	-0.35
Current temp. coeff.	$\beta (\%/K)$	0.058	0.045
Number of Series panels	N_s	8	8
Number of Parallel panels	N_p	2	2
PV array rated power	$P_{array} (W)$	5000	5000
PV array rated MPPT voltage	$V_{array} (V)$	330	380

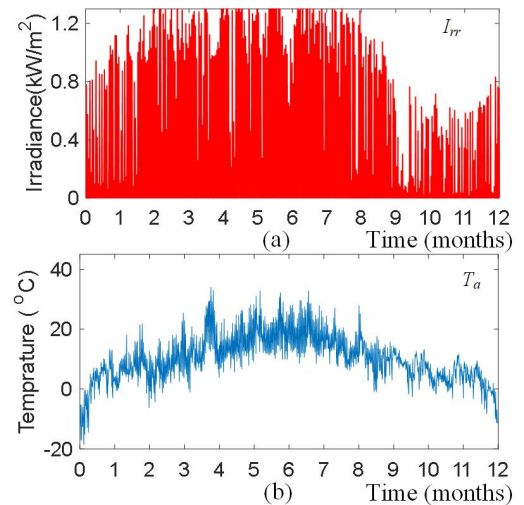


Fig. 3: Measured climate conditions, (a) annual solar irradiance (I_{rr}), and (b) ambient temperature (T_a).

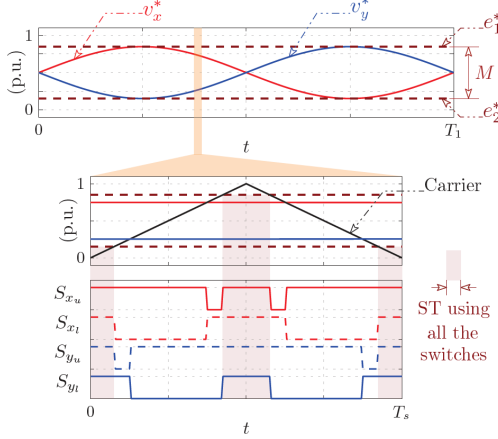


Fig. 4: Utilized modulation scheme of the single-phase qZSI, which is called two-phase-leg ST-based sinusoidal modulation (2P-SM).

In order to operate the qZSI, the ST state has to be properly inserted within the zero states, resulting in no effect on the active states and thereby the output AC voltage. In this paper, the two-phase-leg ST-based sinusoidal modulation (2P-SM) is employed, which is shown in Fig. 4. Using this modulation strategy, the ST state is inserted by comparing e_1^* and e_2^* with the carrier signal, and if the carrier signal is larger than e_1^* or smaller than e_2^* , all the switches are turned ON simultaneously. Otherwise, the B4-bridge is modulated in the conventional way by comparing the sinusoidal reference signals (v_x^* and v_y^*) with the carrier signal. Under this modulation strategy, the ST current is divided between the two phase-legs and the ST state is inserted twice in each switching period. Furthermore, the ST duty cycle is constant and its average value (D_0) is equal to $(1-M)$, where M is the modulation index that is defined in Figure 3. Notably, the Maximum Power Point Tracking (MPPT) control of the PV array can be carried out by suitably controlling the ST duty cycle.

B. Conventional two-stage inverter

The structure of the conventional two-stage inverter is shown in Fig. 2. Comprising a boost-based DC-DC converter and a B4-bridge. The boost stage is in charge of MPPT control of PV arrays and the inverter is feeding the MPPT power into the grid by regulating the DC link voltage.

Both converters are designed considering the same capacity, input ripple current, DC link ripple voltage and AC current Total Harmonic Distortion (THD) in order to make a fair reliability comparison study. The converter parameters and selected components are summarized in Table II. In the following the reliability of both converters are explained.

III. RELIABILITY PREDICTION APPROACH

In this section, the reliability of the converters is estimated according to the mission profile based reliability assessment approach discussed in [13]–[17]. Capacitors and active switches are two of the failure prone components in the power converters. According to [18], the lifetime model of electrolytic capacitors (L_t) is represented by:

Table II: PV inverters parameters

Topology	qZSI	Two-stage Inverter
Capacity	5 kW	5 kW
Inductor (L_b, L_n)	2 mH	2 mH
Switching frequency	10 kHz	10 kHz
DC voltage ripple	10%	10%
Input current ripple	30%	30%
AC current THD	3%	3%
Diode	4×IDP30E65D2 1×IDP30E65D2	4×IDP30E65D2 1×IDP30E65D2
Switch	4×IGW60N60H3	4×IGW60N60H3 1×IGB15N60T
DC link capacitors	5×220 μ F 450 V	2×(3×390) μ F 450 V

$$L_t = L_o \cdot 2^{\frac{T_o - T_t}{n_1}} \left(\frac{V_t}{V_o} \right)^{-n_2} \quad (1)$$

where, L_o is the nominal lifetime under nominal voltage of V_o and nominal capacitor temperature of T_o , and L_t is the capacitor lifetime under voltage of V_t and capacitor temperature of T_t . The constants n_1 and n_2 are provided in [18]. The wear-out failure distribution of electrolytic capacitors is represented in [3] under nominal operating conditions, where it is modled by the Weibull distribution with $\alpha = 6804$ hours and $\beta = 5.12$. For a given mission profile, B_x consumed lifetime $CL(B_x)$ can be found using:

$$CL(B_x) = \sum_k \frac{t_k}{L_{t-k}} (B_x) \quad (2)$$

where t_k is the k^{th} period of mission profile with lifetime of L_{t-k} which can be obtained using (1) under operating conditions of V_t and T_t and B_x lifetime of L_o based on [3]. The failure distribution function of a capacitor under operating condition can be obtained using CL under different B_x lifetimes. The total reliability of a capacitor bank is defined as a series connection of all capacitors from reliability standpoint. The whole procedure of capacitor reliability modeling is shown in Fig. 7.

The number of cycles to failure N_f of semiconductor switches is obtained from (3) according to [19].

$$N_f = A \cdot \Delta T_j^\alpha \cdot \exp\left(\frac{\beta}{T_{jm}}\right) \cdot \left(\frac{t_{on}}{1.5}\right)^{-0.3} \quad (3)$$

where ΔT and T are the junction temperature swing and average respectively, and t_{on} is the rising time of temperature cycle. The constants A , α , and β are curve fitting constants which can be obtained from aging tests [19]. The wear-out failure prediction procedure of semiconductor switches is shown in Fig. 5. This approach has been described in [16], [17], [20], where the mission profile is translated to the temperature of IGBT and diode. The temperature profile is classified into different classes with specific number of cycles, temperature swing, and temperature average. For each class, the damage on the device is determined by dividing the number of cycles by the number of cycles to failure. Therefore, damage

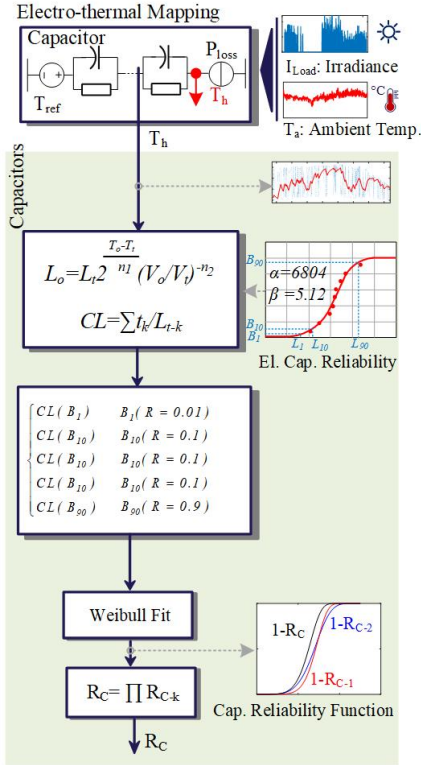


Fig. 7. Mission profile-based wear-out failure prediction procedure of electrolytic capacitors.

distribution under the given mission profile is determined for different classes. It is converted to an equivalent damage with the same impact on the device from stress point of view. The statistics of uncertain parameters on the static damage can be modeled by Monte Carlo simulation, and hence, the failure distribution function is predicted for the given mission profile. The total semiconductor devices reliability is obtained by considering the series connection of them from reliability point of view. Finally, the total converter reliability is calculated by multiplying the reliability of capacitors to the semiconductor devices.

IV. COMPARATIVE ASSESSMENT

The reliability of conventional inverter connected to the PV arrays I and II is shown in Fig. 6 and Fig. 8, respectively. Furthermore, Fig. 9 and Fig. 10 show the qZSI reliability functions with PV arrays I and II.

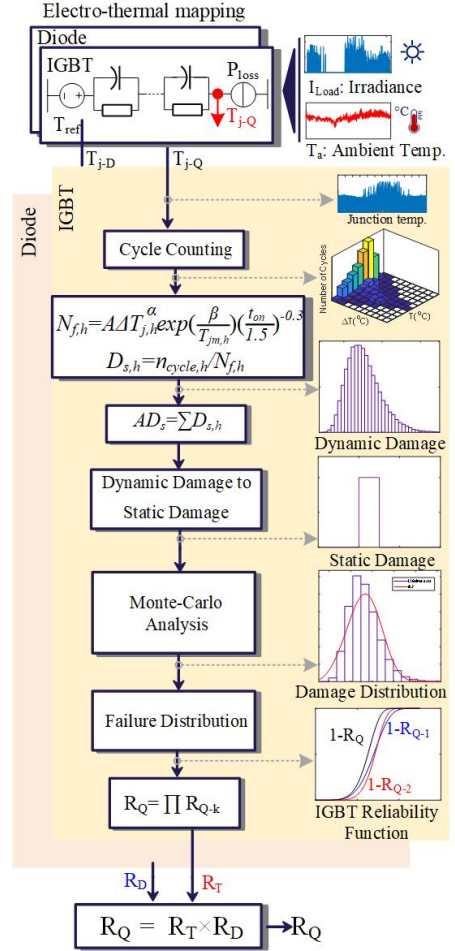


Fig. 5. Mission profile-based wear-out failure prediction procedure of semiconductors.

Following Fig. 6 and Fig. 8, the conventional inverter reliability under given mission profile is almost 99.995% during its 10-year operation. According to the selected switches in Table II, the reliability of active switches are very high as shown in Fig. 6(b) and Fig. 8(b), while the capacitor bank limits the total converter reliability following Fig. 6(a) and Fig. 8(a). Meanwhile, the boost converter diode experiences a bit more stress with PV array II as depicted in Fig. 8(a) due to the fact that it has different duty cycles with the two PV arrays.

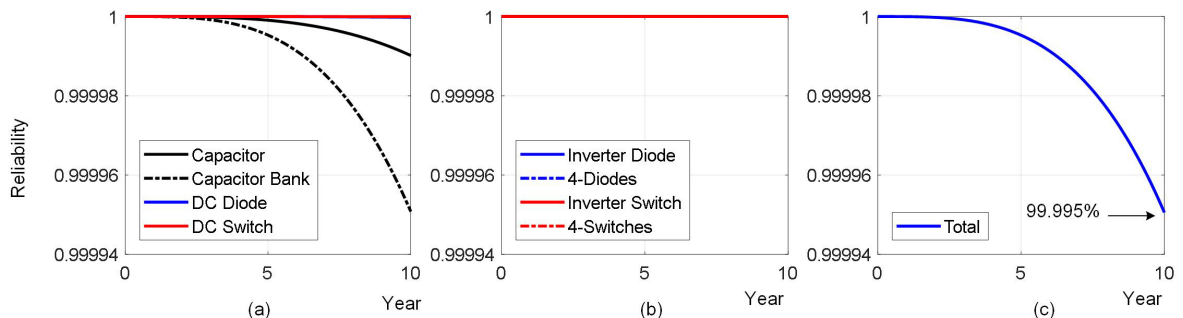


Fig. 6: Obtained Reliability functions of the conventional inverter connected to PV array I, from component-level to converter-level; (a) individual capacitor and capacitor bank, (b) DC side diode, (c) individual diode/IGBT and four diodes/IGBTs of inverter, and (d) total converter reliability functions.

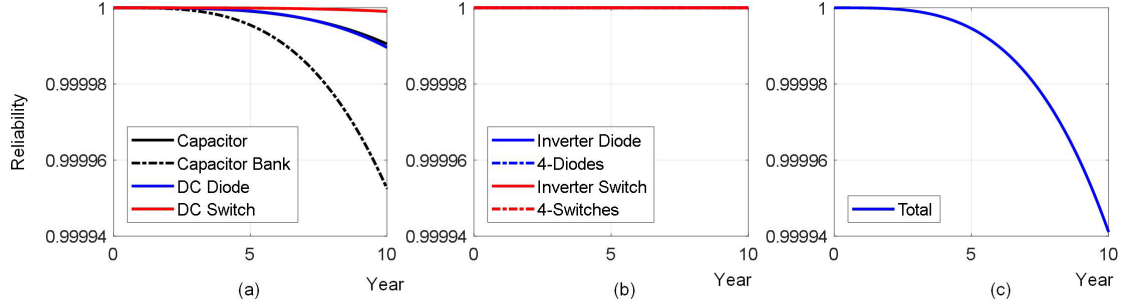


Fig. 8: Obtained Reliability functions of the conventional converter connected to PV array II, from component-level to converter-level; (a) individual capacitor and capacitor bank, (b) DC side diode, (c) individual diode/IGBT and four diodes/IGBTs of inverter, and (d) total converter reliability functions.

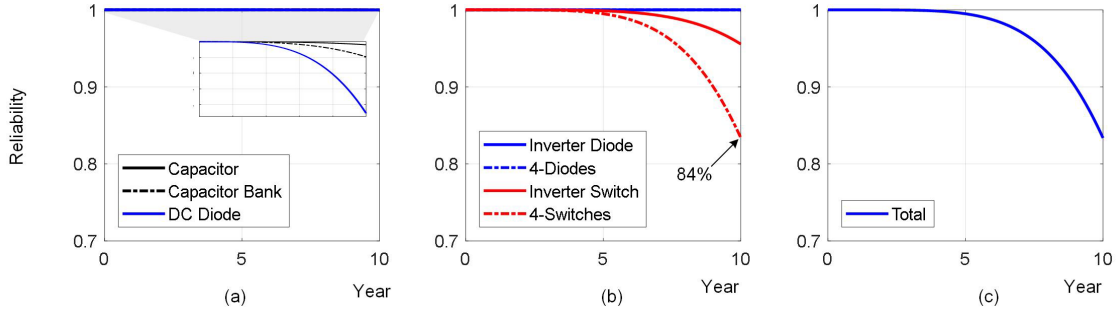


Fig. 9: Obtained Reliability functions of the qZSI connected to PV array I, from component-level to converter-level; (a) individual capacitor and capacitor bank, (b) DC side diode, (c) individual diode/IGBT and four diodes/IGBTs of inverter, and (d) total converter reliability functions.

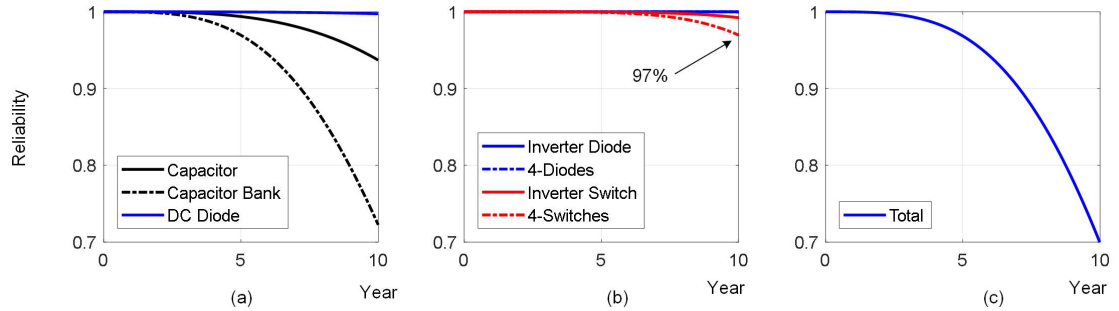


Fig. 10: Obtained Reliability functions of the qZSI connected to PV array II, from component-level to converter-level; (a) individual capacitor and capacitor bank, (b) DC side diode, (c) individual diode/IGBT and four diodes/IGBTs of inverter, and (d) total converter reliability functions.

The reliability of qZSI with PV array I is limited by the inverter switches as seen from Fig. 9(b), while the capacitor bank and DC side diode have better reliability as shown in Fig. 9(a). However, employing PV array II introduces less stress on the inverter switches as shown in Fig. 10(b). This fact is associated with the qZSI control principle, where the higher input voltage (PV array II) causes lower ST duty cycle and lower AC current at the constant PV power as shown in Fig. 11(a) for a rated operation condition. Employing PV array II induces small ST (see Fig. 11 for different operation points), small DC and AC currents, hence the stress on the inverter switches will be decreased. For instance, the reliability of inverter switches (4-switches) is 84% for array I, and 97% for array II during 10-year operation. On the contrary, stress on the capacitor bank in the presence of array II is increased and it limits the qZSI reliability as shown in Fig. 10(a, c).

Considering the same design criteria – i.e., inverter capacity, input current ripple, DC link voltage ripple, and AC current harmonics – for both inverters, the conventional inverter has better reliability as shown in the reported results in this section. Two factors are

deteriorating the qZSI reliability compared to the conventional inverter. Firstly, since the inverter is responsible for boosting the input DC voltage and feeding it into grid, the current of inverter switches in qZSI during ST state is greater than that of in conventional inverter as shown in Figure 10 for a rated operating condition. Secondly, the effective switching frequency of qZSI is two times of the conventional inverter as shown in Figure 10. These factors increase the stress of the switches. For instance, as shown in Fig. 6(b) and Fig. 9(b), the reliability of switches is almost 100% for conventional inverter and 83% for qZSI.

In order to improve the qZSI, the ST can be decreased by selecting suitable and applicable PV array connection with higher MPPT voltages. By doing so, the inverter switches reliability is enhanced from 83% to 97% respectively for PV arrays I and II as shown in Fig. 9(b) and Fig. 10(b). Meanwhile, the capacitor bank reliability is decreased as shown in Fig. 10(a), hence it should be redesigned according to the corresponding PV array. Even though a redesigned capacitor bank with a higher reliability cannot make the qZSI to compete with the conventional one from the reliability perspective. This fact

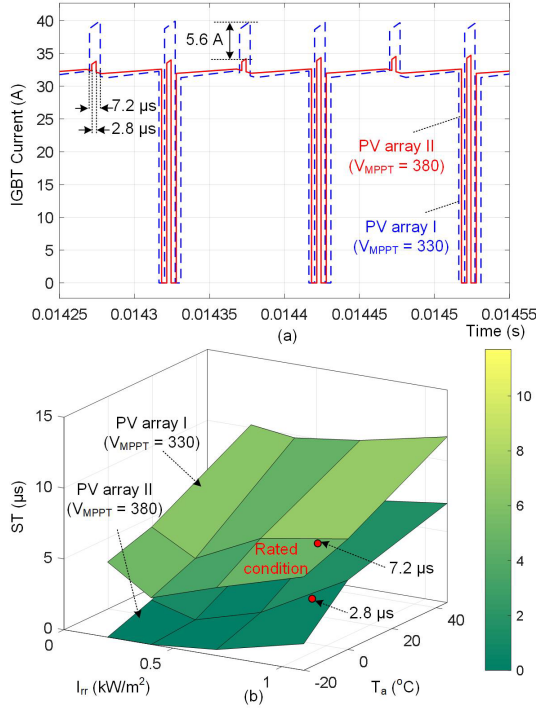


Fig. 11: Inverter IGBT peak current operating at irradiance of 1000 W/m² and PV cell temperature of 25 °C; (a) Shoot Through (ST) of qZSI in terms of climate conditions considering PV arrays I and II, (b) showing the impact of PV array on the peak current of qZSI.

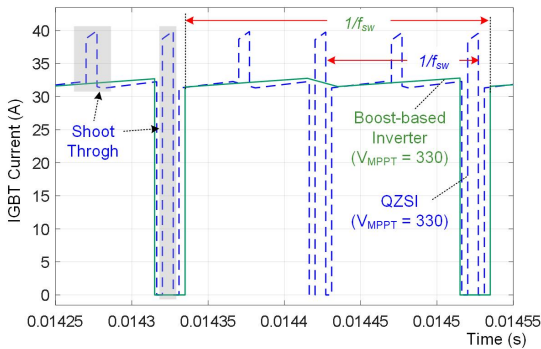


Fig. 12: Comparing peak current of conventional inverter with qZSI with PV array I at STC (irradiance of 1000 W/m² and PV cell temperature of 25 °C).

can be deduced by comparing the reliability of qZSI switches in Fig. 10(b) with the total conventional inverter reliability shown in Fig. 8(c). Therefore, even if the capacitor bank reliability was almost 1, the total qZSI reliability would be 97%, while the total reliability of conventional inverter is almost 99.995%.

V. CONCLUSION

This paper presents a reliability comparison between a single-phase quasi-Z-Source Inverter (qZSI) and a conventional two-stage boost-based inverter for grid-tied PV applications. A mission profile-based reliability assessment approach is employed to model the inverters reliability considering the wear-out failure of the two fragile components, i.e., semiconductor devices and capacitors. Despite the fact that the main merit behind utilizing qZSI (impedance source converter) is to

eliminate the boost stage, but the obtained analysis has revealed that, the conventional two-stage boost-based inverter poses higher reliability. Furthermore, the impact of Shoot Trough (ST) state on the qZSI reliability is investigated by selecting different PV arrays, where a suitable PV array design can improve the converter reliability.

REFERENCES

- [1] "Solar PV Grew Faster than Any Other Fuel in 2016, Opening a New Era for Solar Power," *International Energy Agency*, 2017. [Online]. Available: <https://www.iea.org/>. [Accessed: 25-Jul-2018].
- [2] H. Wang, K. Ma, and F. Blaabjerg, "Design for Reliability of Power Electronic Systems," *IECON 2012 - 38th Annu. Conf. IEEE Ind. Electron. Soc.*, pp. 33–44, Oct. 2012.
- [3] D. Zhou, H. Wang, and F. Blaabjerg, "Mission Profile Based System-Level Reliability Analysis of DC/DC Converters for a Backup Power Application," *IEEE Trans. Power Electron.*, vol. 33, no. 9, pp. 8030–8039, 2018.
- [4] F. Z. Peng, "Z-Source Inverter," *IEEE Trans. Ind. Appl.*, vol. 39, no. 2, pp. 504–510, Mar. 2003.
- [5] A. Abdelhakim, P. Davari, F. Blaabjerg, and P. Mattavelli, "An Improved Modulation Strategy for the Three-Phase Z-Source Inverters (ZSIs)," in *Proc. IEEE ECCE*, 2017, pp. 4237–4243.
- [6] M. Mohr, W. T. Franke, B. Wittig, and F. W. Fuchs, "Converter Systems for Fuel Cells in the Medium Power Range—A Comparative Study," *IEEE Trans. Ind. Electron.*, vol. 57, no. 6, pp. 2024–2032, Jun. 2010.
- [7] M. Zdanowski, D. Pefitsis, S. Piasecki, and J. Rabkowski, "On the Design Process of a 6-KVA Quasi-Z-Inverter Employing SiC Power Devices," *IEEE Trans. Power Electron.*, vol. 31, no. 11, pp. 7499–7508, Nov. 2016.
- [8] A. Abdelhakim, P. Davari, F. Blaabjerg, and P. Mattavelli, "Switching Loss Reduction in the Three-Phase Quasi-Z-Source Inverters Utilizing Modified Space Vector Modulation Strategies," *IEEE Trans. Power Electron.*, vol. 33, no. 5, pp. 4045–4060, May 2018.
- [9] Y. Liu, H. Abu-Rub, and B. Ge, "Z-Source/Quasi-Z-Source Inverters: Derived Networks, Modulations, Controls, and Emerging Applications to Photovoltaic Conversion," *IEEE Ind. Electron. Mag.*, vol. 8, no. 4, pp. 32–44, Dec. 2014.
- [10] Y. Zhou, L. Liu, and H. Li, "A High-Performance Photovoltaic Module-Integrated Converter (MIC) Based on Cascaded Quasi-Z-Source Inverters (QZSI) Using EGSN FETs," *IEEE Trans. Power Electron.*, vol. 28, no. 6, pp. 2727–2738, Jun. 2013.
- [11] B. Ge, H. Abu-Rub, F. Z. Peng, Q. Lei, A. T. de Almeida, F. J. T. E. Ferreira, D. Sun, and Y. Liu, "An Energy-Stored Quasi-Z-Source Inverter for Application to Photovoltaic Power System," *IEEE Trans. Ind. Electron.*, vol. 60, no. 10, pp. 4468–4481, Oct. 2013.
- [12] F. Guo, L. Fu, C.-H. Lin, C. Li, W. Choi, and J. Wang, "Development of an 85-KW Bidirectional Quasi-Z-Source Inverter With DC-Link Feed-Forward Compensation for Electric Vehicle Applications," *IEEE Trans. Power Electron.*, vol. 28, no. 12, pp. 5477–5488, Dec. 2013.
- [13] Y. Shen, A. Chub, H. Wang, D. Vinnikov, E. Liivik, and F. Blaabjerg, "Wear-out Failure Analysis of an Impedance-Source PV Microinverter Based on System-Level Electro-Thermal Modeling," *IEEE Trans. Ind. Electron.*, no. Early Access (10.1109/TIE.2018.2831643), 2018.
- [14] P. D. Reigosa, H. Wang, Y. Yang, and F. Blaabjerg, "Prediction of Bond Wire Fatigue of IGBTs in a PV Inverter under a Long-Term Operation," *IEEE Trans. Power Electron.*, vol. 31, no. 10, pp. 3052–3059, Mar. 2016.
- [15] T. Loix, R. Belmans, and K. U. Leuven, "A Three-Phase Voltage and Frequency Droop Control Scheme for Parallel Inverters," *Ind. Electron.*, vol. 22, no. 1, pp. 1662–1667, 2007.
- [16] S. Peyghami, H. Wang, P. Davari, and F. Blaabjerg, "Mission Profile Based Power Converter Reliability Analysis in a DC Power Electronic Based Power System," in *Proc. IEEE ECCE*, 2018, pp. 1–7.
- [17] S. Peyghami, P. Davari, H. Wang, and F. Blaabjerg, "The Impact

of Topology and Mission Profile on the Reliability of Boost-Type Converters in PV Applications,” in *Proc. IEEE COMPEL*, 2018, pp. 1–8.

- [18] A. Albertsen, “Electrolytic Capacitor Lifetime Estimation,” *JIANGHAI Eur. GmbH*, pp. 1–13, 2010.
- [19] R. Bayerer, T. Herrmann, T. Licht, J. Lutz, and M. Feller, “Model for Power Cycling Lifetime of IGBT Modules - Various Factors Influencing Lifetime,” in *Proc. IEEE CIPS*, 2008, pp. 1–6.
- [20] S. Peyghami, P. Davari, H. Wang, and F. Blaabjerg, “System-Level Reliability Enhancement of DC/DC Stage in a Single-Phase PV Inverter,” *Microelectron. Reliab.*, vol. 88–90, pp. 1030–1035, Sep. 2018.